Contrasting origins of the upper mantle revealed by hafnium and lead isotopes from the Southeast Indian Ridge

Barry B. Hanan[1], Janne Blichert-Toft[2], Douglas G. Pyle[3] & David M. Christie[4]

[1]*Department of Geological Sciences, San Diego State University, 5500 Campanile Drive, San Diego, California 92182-1020, USA*
[2]*Ecole Normale Superieure de Lyon, Laboratoire des Sciences de la Terre, CNRS UMR 5570, 46 Allee d'Italie, 69364 Lyon Cedex 7, France*
[3]*School of Ocean and Earth Science Technology, University of Hawaii, 1680 East-West Road, POST 612A, Honolulu, Hawaii 96822, USA*
[4]*College of Oceanic and Atmospheric Sciences, Oregon State University, 104 COAS Admin Bldg, Corvallis, Oregon 97331-5503, USA*

The origin of the isotopic signature of Indian mid-ocean ridge basalts has remained enigmatic, because the geochemical composition of these basalts is consistent either with pollution from recycled, ancient altered oceanic crust and sediments, or with ancient continental crust or lithosphere. The radiogenic isotopic signature may therefore be the result of contamination of the upper mantle by plumes containing recycled altered ancient oceanic crust and sediments[1], detachment and dispersal of continental material into the shallow mantle during rifting and breakup of Gondwana[2], or contamination of the upper mantle by ancient subduction processes[3,4]. The identification of a process operating on a scale large enough to affect major portions of the Indian mid-ocean ridge basalt source region has been a long-standing problem. Here we present hafnium and lead isotope data from across the Indian–Pacific mantle boundary at the Australian–Antarctic discordance region of the Southeast Indian Ridge, which demonstrate that the Pacific and Indian upper mantle basalt source domains were each affected by different mechanisms. We infer that the Indian upper-mantle isotope signature in this region is affected mainly by lower continental crust entrained during Gondwana rifting, whereas the isotope signature of the Pacific upper mantle is influenced predominantly by ocean floor subduction-related processes.

Geochemists have identified five types of mantle reservoirs on the basis of radiogenic isotope tracers[5]. One, the depleted asthenosphere mid-ocean ridge basalts (MORB) mantle source (DM[6]) is variably polluted on a regional scale by at least two of these isotopically distinct components[7,8]. One, C-like[8], is typified by intermediate $^{206}Pb/^{204}Pb$, the other, EM-1-like and EM-2-like or DUPAL-like[6–8], can have very low $^{206}Pb/^{204}Pb$. The marked contrast in the radiogenic isotope signatures between Indian and Pacific MORB is attributed to a greater proportion of an EM-1-like component, with very low $^{206}Pb/^{204}Pb$ and positive $\Delta^{207}Pb$ and $\Delta^{208}Pb$ (ref. 9), in the Indian upper mantle[8]. The origin of the EM-1-like material may represent ancient subcontinental lithospheric mantle (SCLM) or ancient recycled oceanic crust and sediment[4,10–12].

The known Indian Ocean plumes are too enriched in radiogenic Pb isotopes to account for the distinctly lower $^{206}Pb/^{204}Pb$ of Indian MORB relative to Pacific MORB[4]. The low trace-element abundances of SCLM, which require very large amounts for it to be an effective contaminant, and average $^{187}Os/^{186}Os$ ratios that are significantly lower than depleted MORB, also do not support SCLM as the origin of the EM-1 signature[4,13]. The alternative remaining options for the Indian MORB EM-1 isotopic signature are thus sediment and altered oceanic crust accreted to the continent before being mixed into the upper-mantle MORB source[2], recycled material stored at a mantle boundary layer[12], or mantle wedge contamination by subducting slabs[3]. Here we present new Hf

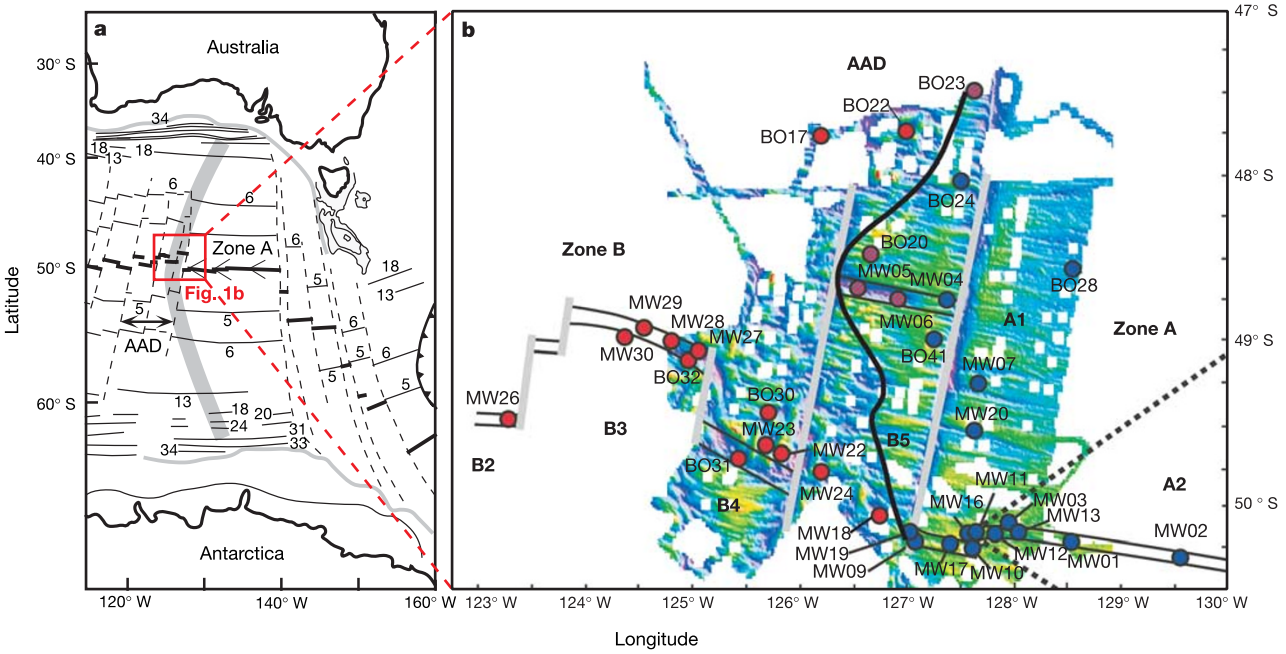

Figure 1 Regional setting of the AAD along the SEIR between Australia and Antarctica, schematic tectonic summary, and sample dredge locations. **a**, Transform fault zones (thin dashed lines) and magnetic lineations (solid lines) are shown. The broad grey curved line represents the regional depth anomaly[16] that is at present associated with the AAD. The off-axis trace of the isotopic boundary lies within the eastern half of the depth anomaly (see Supplementary Information for the references used to compile Fig. 1a). **b**, Sample locations for the sample data shown in Supplementary Table 1 are shown on the Seabeam bathymetry of the AAD region of the SEIR[16]: blue circles, Pacific-type; red circles, Indian-type; cross-hatched circles, transitional mantle sources. (Sample numbers with prefixes MW and BO correspond to the sample names in Supplementary Table 1) The ridge axis is bounded by the thin black lines. Fracture zones are represented by the thick grey lines. The approximate location of the AAD mantle boundary is indicated by the wavy black line.

and Pb isotope data for zero-age[14] and off-axis basalt glasses from the Southeast Indian Ridge (SEIR)[15,16] that support a model in which the shallow mantle in the Australian–Antarctic discordance (AAD) region was polluted by lower continental crust during rifting and breakup of Gondwana.

The AAD is the location of a geochemical and tectonic boundary between the Indian and Pacific upper-mantle provinces (Fig. 1). The deepest contiguous segments of the global mid-ocean ridge system lie within the AAD. The AAD and associated depth anomaly are an expression of cool upper mantle that has persisted since the separation of Australia from Antarctica during Gondwana breakup about 50 Myr ago. The origin of the depth anomaly has been variously attributed to a fragment of foundered SCLM, a stagnated subducted slab, or convective downwelling beneath the SEIR[16].

The sharp mantle boundary occurs over a few tens of kilometres[3,14–17]. Compared to zone A1–2 Pacific MORB from east of the AAD, zone B2–4 Indian MORB to the west have lower $^{206}Pb/^{204}Pb$ values combined with higher $\Delta^{208}Pb$ and $\Delta^{207}Pb$ values, and more radiogenic $^{87}Sr/^{86}Sr$, all characteristics of strong influence from an EM-1 mantle source component. The range in ε_{Hf} is similar on both sides of the mantle discontinuity from about 123°–130° E (refs 3, 17), except for the zone B4 segment, which has the most ultra-depleted Hf isotope compositions reported so far for MORB worldwide[17]. A step-like discontinuity is visible in the $\Delta\varepsilon_{Hf}$ trend ($\Delta\varepsilon_{Hf}$ correlates with increasing source depletion) from higher values (>1) on the Indian side of the boundary to lower values (<1) on the Pacific side (Supplementary Fig. 1). Basalts from zone B5, adjacent to the AAD boundary, derive from a mixture of Indian and Pacific mantle. These basalts have radiogenic isotope compositions transitional between zone B Indian and zone A Pacific MORB[3,14,17].

The C-like component, with intermediate Pb, Sr, Nd and Hf isotope ratios (for example, C[8] or FOZO[18] mantle components) relative to oceanic island basalts and MORB, is thought to derive from the deep mantle via hotspot mantle plumes[5]. The low-$^{206}Pb/^{204}Pb$ EM-1-like component has isotope characteristics typical of recycled ancient oceanic sediment or SCLM[11,19]. Binary-like arrays for the Pacific, Atlantic and Indian MORB subpopulations converge towards the intermediate component C at relatively higher $^{206}Pb/^{204}Pb$, but are distinguished at low $^{206}Pb/^{204}Pb$ by differences in their relative proportions of the DM and EM-1 components[8]. In the AAD the contrast between Pacific and Indian MORB is striking in the ε_{Hf}–$^{206}Pb/^{204}Pb$ diagram (Fig. 2a), in which there is no overlap between zone A and zone B MORB, except for the transitional, mixed-source basalts[3,17]. Zone A basalts define a tight cluster with relatively low ε_{Hf} and $^{206}Pb/^{204}Pb$ and fall along a

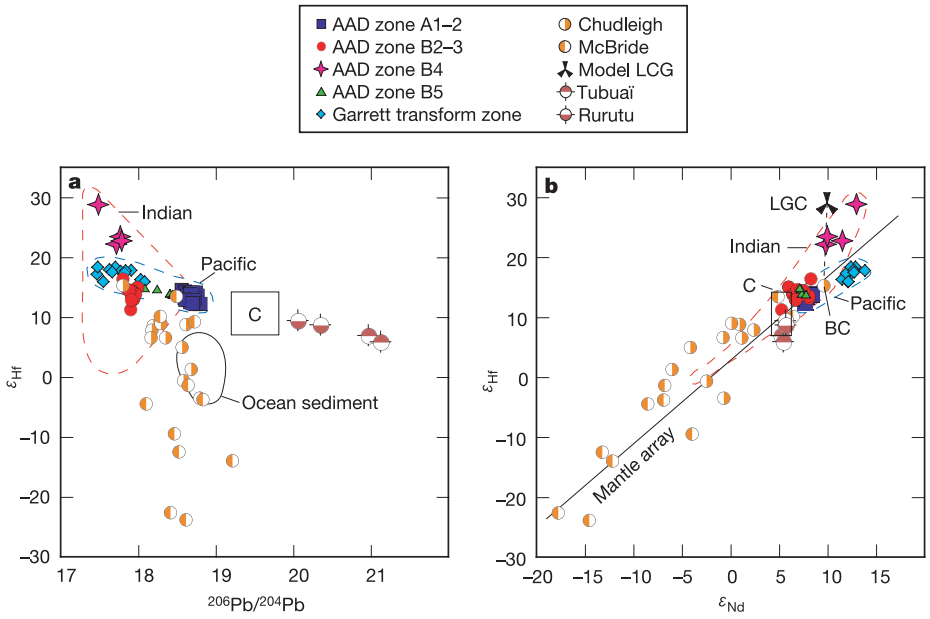

Figure 2 The ε_{Hf}, ε_{Nd} and $^{206}Pb/^{204}Pb$ variations of MORB from the AAD region of the SEIR. **a**, Pacific MORB from zone A1–2 fall on an array with ultra-depleted MORB[20] (J. Blichert-Toft and C. Hemond, personal communication) from the Garrett transform zone, the common component C[8], and Pacific HIMU ocean island basalts[22] from Tubuaï and Rurutu. Indian zone B2–4 MORB define a separate array oblique to the Pacific array and include lower crustal granulites from Australia[25,26]. The field for Pacific and Indian oceanic sediment[27,28] overlaps with the Australian xenoliths. The fields for Pacific and Indian fields include the AAD zone B2–4 and zone A1–2 data and the MORB data from Chauvel and Blichert-Toft[21]. Note that in **b** the ultra-depleted Garrett transform zone and zone B4 basalts have completely overlapping ranges in ε_{Nd}. In a plot of $^{206}Pb/^{204}Pb$ versus ε_{Nd}, the Pacific and Indian trends do not cross, but intersect at the depleted ends of their arrays. This indicates that the two sources had similar time-integrated histories with respect to Sm/Nd, but marked differences in Lu/Hf fractionation. In this $^{206}Pb/^{204}Pb$–ε_{Hf} projection the AAD zone A and other Pacific MORB[21] define a linear trend but the AAD zone B2–4 and other Indian MORB[21] together define a triangular shaped field that narrows and converges towards the C component[8]. In contrast, the Indian and Pacific trends are both linear-like and converge towards the C component in Pb isotope space. The range in ε_{Hf} increases with decreasing $^{206}Pb/^{204}Pb$ consistent with the idea that the low $^{206}Pb/^{204}Pb$ component in Indian MORB results from pollution of the regular upper-mantle MORB source with a lower crustal granulite (LCG) component with a wide range of time-integrated Lu/Hf. The linear-like array shown by the AAD zone B2–4 data, within the Indian field, is dominated by the local heterogeneity. In Pb–Pb isotope correlations, the global Indian MORB population also shows relatively more dispersion (that is, heterogeneity) in $^{207}Pb/^{204}Pb$ and $^{208}Pb/^{204}Pb$ at a given low $^{206}Pb/^{204}Pb$ than the Pacific MORB population, consistent with a larger proportion of EM-1-like continental crustal component in the Indian upper-mantle MORB source. **b**, The Indian ultra-depleted MORB from zone B4 plot on or above the ε_{Nd}–ε_{Hf} mantle array line of Chauvel and Blichert-Toft[21], whereas the Pacific Garrett transform zone ultra-depleted MORB fall on or below it. In general, except for the transitional zone-B5 mixed-source data, Pacific MORB have lower ε_{Hf} at the same ε_{Nd} than do Indian MORB. The black symbol represents the model composition of LCG depleted by early melting during the initiation of rifting 50 Myr ago. Sample BC, a mafic garnet granulite from the Chudleigh volcanic province, was used for the initial ε_{Hf} and ε_{Nd} isotope compositions[25,26]. Values for Lu/Hf of 3.0 and Sm/Nd of 0.5 were assumed for the residue after melting. These parent/daughter trace-element ratios are in the range observed for the garnet granulite xenoliths from the Kilbourne Hole[29]. The model data point (LCG), representing the residue, evolves about 14 ε_{Hf} units compared to less than one ε_{Nd} unit in 50 Myr. The dashed line connects the model LCG point and the starting material, sample BC.

typical Pacific MORB–ocean island basalt trend defined by the most depleted Pacific MORB from the Garrett transform zone[20] (J. Blichert-Toft and C. Hemond, personal communication), regular Pacific MORB[21], the intermediate component C[8] and Pacific HIMU[6] (an enriched mantle component with high $\mu = {}^{238}U/{}^{204}Pb$) oceanic island basalts[22]. In contrast, zone B2–4 Indian MORB define a prominent negative trend oblique to and cross-cutting the Pacific trend. All reported Pacific MORB, including the ultra-depleted basalts from the Garrett transform zone, plot very near ($\Delta\varepsilon_{Hf} < 1$) or below the mantle array in ε_{Nd}–ε_{Hf} space, whereas the ultra-depleted basalts from zone B4 in the AAD and most Indian MORB plot on or above it ($\Delta\varepsilon_{Hf} > 1$) (Figs 2b and 3).

The contrast between the Indian and Pacific isotope signatures could result from long-term differences in parent/daughter ratios related to the relative timing of melting events in an originally homogeneous upper mantle. Alternatively, the isotopic contrasts may be interpreted as evidence of melting of lithologically heterogeneous upper mantle. For example, the isotopic compositions of MORB and associated abyssal peridotites from the Southwest Indian Ridge show that a component other than peridotite is required to explain the enriched end of the range of variation in ε_{Nd} observed in these basalts[23]. This component may be pyroxenite or eclogite[23] having a lower melting temperature than peridotite. The contrasting Indian and Pacific linear MORB trajectories in multi-isotope space are consistent with pollution and mixing of different recycled components within the upper-mantle MORB source regions over time[8]. In the $^{206}Pb/^{204}Pb$–ε_{Hf} diagram, zone A MORB fall along the Pacific trend. A two-component mantle consisting of pyroxenite or ecologite with a C-like isotope signature embedded in peridotite with a Garrett-transform-zone-like ultra-depleted isotope signature could yield first melts with zone-A-like composition, and, upon further melting, Garrett transform zone basalts.

Because the mineralogy of the Indian and Pacific MORB mantle sources are expected to be similar (pyroxene initially on the liquidus and similar trace-element abundance ratios), mantle mixing trends are linear rather than hyperbolic[24], implying that the enriched component in the Indian source should lie on the high-$^{206}Pb/^{204}Pb$ extension of the linear array defined by the zone B2–4 data. Because the zone B2–4 array cuts across the Pacific trend, the enriched component of the Indian trend must have an isotope signature distinct from the enriched C-like or HIMU signature observed for the Pacific. Possible end-members include lower crust, such as represented by mafic granulite xenoliths from the nearby Chudleigh and McBride volcanic provinces of Australia[25,26], or oceanic sediment[27,28]. The low-$^{206}Pb/^{204}Pb$ end of the Indian trend is also distinct from the Pacific trend. In contrast to the ε_{Hf}–$^{206}Pb/^{204}Pb$ diagram, a plot of $^{206}Pb/^{204}Pb$ versus ε_{Nd} for the Pacific and Indian trends shows that these two arrays intersect at their depleted ends. Thus the two sources have had similar time-integrated histories with respect to Sm/Nd, but have experienced marked differences in Lu/Hf fractionation. Observations from a well-known incipient continental rift tectonic environment, the Rio Grande Rift, offer an explanation for the high-ε_{Hf} end-member and support the model for contamination of the Indian AAD upper mantle by lower crust.

Anomalously high $\Delta\varepsilon_{Hf}$ values, such as those of the Indian MORB zone B4 samples, require a time-integrated Lu/Hf source composition substantially different from that of all other known oceanic basalt mantle sources, including both MORB and ocean island basalts. Garnet granulite xenoliths from the Kilbourne Hole, which represent residues from early magmatic processes during the initiation of the Rio Grande Rift around 25 Myr ago, have extremely high Lu concentrations and Lu/Hf ratios of 6.5–9.1 (ref. 29). The zone B4 ultradepleted component would require a comparatively much lower Lu/Hf ratio of only about 3 to develop its ε_{Hf} of about 30 from melting of Australian granulite-like material in 50 Myr (Fig. 2b). The high-ε_{Hf}, low-$^{206}Pb/^{204}Pb$ end-member of the AAD zone B2–4 MORB array would thus be consistent with the melting of lower crustal granulite followed by the incorporation of the residues into the MORB mantle source during initial rifting about 50 Myr ago.

The origin of the low-$^{206}Pb/^{204}Pb$ EM-1 (and relatively higher-$^{206}Pb/^{204}Pb$ EM-2) signature in oceanic basalt may derive from continental crust or lithospheric mantle and/or sediment pollution. For the AAD, detachment and dispersal of continental lower crust into the shallow mantle during the rifting and breakup of Gondwana adequately accounts for the EM-1-like pollution of the zone B2–4 Indian MORB mantle source on the SEIR. We exclude recycled sediments as an alternative explanation for the EM-1 component in the Indian MORB mantle source for the following reason. Whereas strong EM-1 signatures are characteristic of Indian and South Atlantic mid-ocean ridges formed concomitantly with continental rifting and opening of these ocean basins, they are uncommon in the Pacific, which is an ocean basin not associated with continental rifting. Yet the Pacific is a region where recycling of oceanic crust and sediments occurs, largely in association with subduction and plume activity, and EM-2–C–HIMU isotopic signatures predominate. The contrast between the most depleted MORB from the Pacific Garrett transform zone MORB and Indian AAD zone B4 MORB requires a process that decouples the Lu–Hf and Sm–Nd systems in EM-1-like mantle material. This is a characteristic of rifting of lower crust, not of Pacific-style subduction and/or plume-related recycling. We also rule out pollution of the AAD Indian MORB source by subduction-modified mantle material forced into the Indian AAD upper mantle by a rising stagnated slab[3]. The $^{3}He/^{4}He$ of the ultra-depleted zone B4 basalts are among the highest reported for MORB away from hotspot influence (8.8 R/R_A; D. Graham, personal communication), not low as would be expected for a subduction-related component[3]. Furthermore, the low $^{206}Pb/^{204}Pb$ ratios of the Indian AAD zone B2–4 MORB are not readily explained by pollution with components derived from Pacific altered oceanic crust and upper crustal sediment shed from Gondwana during the Cretaceous period, when the subducted oceanic crust was located just east of the Australian continental margin[30]. The model for pollution of the AAD MORB source by lower crust may be applicable to other Indian MORB[11,12], to South Atlantic MORB[31], the Arctic Gakkel ridge[32], and to other

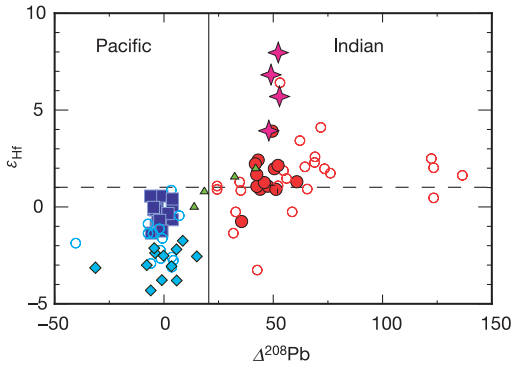

Figure 3 Contrasting $\Delta^{208}Pb$ and ε_{Hf} isotopic variations for MORB from the AAD (this work) and the Indian Ocean basin[21] in general, versus the Pacific Ocean basin[21]. Pacific MORB have $\Delta^{208}Pb < 20$, while Indian MORB have $\Delta^{208}Pb > 20$. In terms of ε_{Hf}, the Pacific data are confined to the southwest quadrant of the diagram with $\varepsilon_{Hf} < 1$. Indian MORB show a large range in ε_{Hf}, both positive and negative, but for the most part plot in the northeast quadrant with $\varepsilon_{Hf} > 1$. The distinction between the Pacific and Indian MORB derives from pollution of the mantle source of the latter by continental crust. The light blue and red open circle symbols are Pacific and Indian MORB[21], respectively. Other symbols are the same as in Fig. 2.

MORB that have formed in conjunction with continental rifting and where EM-1 component signatures occur. □

Received 8 March; accepted 17 September 2004; doi:10.1038/nature03026.

1. Storey, M. *et al.* Contamination of the Indian Ocean asthenosphere by the Kerguelen-Heard mantle plume. *Nature* **338,** 574–576 (1989).
2. Arndt, N. T. & Goldstein, S. L. An open boundary between lower continental crust and mantle: its role in crust formation and crustal recycling. *Tectonophysics* **161,** 210–212 (1989).
3. Kempton, P. D., Pierce, J. A., Barry, T. L., Langmuir, C. & Christie, D. M. Sr-Nd-Pb-Hf isotope results from ODP Leg 187: Evidence for mantle dynamics of the Australian-Antarctic discordance and origin of the Indian MORB source. *Geochem. Geophys. Geosyst.* **3,** doi:10.1029/2002GC000320 (2002).
4. Rehkämper, M. & Hofmann, A. W. Recycled ocean crust and sediment in Indian Ocean MORB. *Earth Planet. Sci. Lett.* **147,** 93–106 (1997).
5. Hofmann, A. W. Mantle geochemistry: the message from oceanic volcanism. *Nature* **385,** 219–229 (1997).
6. Zindler, A. & Hart, S. R. Chemical geodynamics. *Annu. Rev. Earth Planet. Sci.* **14,** 493–571 (1986).
7. Allègre, C. J., Hamelin, B., Provost, A. & Dupré, B. Topology in isotopic mutlispace and the origin of mantle chemical heterogeneities. *Earth Planet. Sci. Lett.* **81,** 319–337 (1986/87).
8. Hanan, B. B. & Graham, D. W. Lead and helium isotope evidence from oceanic basalts for a common deep source of mantle plumes. *Science* **272,** 991–995 (1996).
9. Hart, S. R. A large-scale isotope anomaly in the Southern Hemisphere mantle. *Nature* **309,** 753–757 (1984).
10. Hamelin, B. & Allègre, C.-J. Large-scale regional units in the depleted upper mantle revealed by an isotope study of the South-West Indian Ridge. *Nature* **315,** 196–199 (1985).
11. Mahoney, J. J., Nicollet, C. & Dupuy, C. Madagascar basalts: tracking oceanic and continental sources. *Earth Planet. Sci. Lett.* **104,** 350–363 (1991).
12. Mahoney, J. J., White, W. M., Upton, B. G. J., Neal, C. R. & Scrutton, R. A. Beyond EM-1: lavas from Afanasy-Nikitin rise and the Crozet archipelago, Indian Ocean. *Geology* **24,** 615–618 (1996).
13. Pearson, D. G. *et al.* Archaean Re-Os age for Siberian eclogites and constraints on Archaean tectonics. *Nature* **374,** 711–713 (1995).
14. Pyle, D. G., Christie, D. M. & Mahoney, J. J. Resolving an isotope boundary within the Australian-Antarctic discordance. *Earth Planet. Sci. Lett.* **112,** 161–178 (1992).
15. Pyle, D. G., Christie, D. M., Mahoney, J. J. & Duncan, R. A. Geochemistry and geochronology of ancient southeast Indian and southwest Pacific seafloor. *J. Geophys. Res.* **100,** 22261–22282 (1995).
16. Christie, D. M., West, B. P., Pyle, D. G. & Hanan, B. B. Chaotic topography, mantle flow and mantle migration in the Australian-Antarctic discordance. *Nature* **394,** 637–644 (1998).
17. Hanan, B. B., Blichert-Toft, J., Christie, D. M. & Albaréde, F. Ultra-depleted hafnium isotopes from Australian-Antarctic discordance MORB. *J. Conf. Abstr.* **5** (2), 478–479 (2000).
18. Hart, S. R., Hauri, E. H., Oschmann, L. A. & Whitehead, J. A. Mantle plumes and entrainment: isotopic evidence. *Science* **256,** 517–520 (1992).
19. Weaver, B. L. The origin of ocean island basalt end-member compositions: trace element and isotopic constraints. *Earth Planet. Sci. Lett.* **104,** 381–397 (1991).
20. Wendt, J. I., Regelous, M., Niu, Y., Hekinian, R. & Collerson, K. D. Geochemistry of lavas from the Garrett transform fault; insights into mantle heterogeneity beneath the eastern Pacific. *Earth Planet. Sci. Lett.* **173,** 271–284 (1999).
21. Chauvel, C. & Blichert-Toft, J. A hafnium isotope and trace element perspective on melting of the depleted mantle. *Earth Planet. Sci. Lett.* **190,** 137–151 (2001).
22. Salters, V. J. M. *et al.* Hf isotope constraints on mantle evolution Geochemical Earth Reference Model (GERM). *Chem. Geol.* **145,** 447–460 (1998).
23. Salters, V. J. M. & Dick, H. J. B. Mineralogy of the mid-ocean-ridge basalt source from neodymium isotopic composition of abyssal peridotites. *Nature* **418,** 68–72 (2002).
24. Hart, S. R., Gerlach, D. C. & White, W. M. A possible new Sr-Nd-Pb mantle array and consequences for mantle mixing. *Geochim. Cosmochim. Acta* **50,** 1551–1557 (1986).
25. Rudnick, R. L. & Goldstein, S. L. The Pb isotopic compositions of lower crustal xenoliths and evolution of lower crustal Pb. *Earth Planet. Sci. Lett.* **98,** 192–207 (1990).
26. Vervoort, J. D. *et al.* Hf-Nd isotopic evolution of the lower crust. *Earth Planet. Sci. Lett.* **181,** 115–129 (2000).
27. Ben Othman, D., White, W. M. & Patchett, P. J. The geochemistry of marine sediments, island arc magma genesis, and crust-mantle recycling. *Earth Planet. Sci. Lett.* **94,** 1–21 (1989).
28. Vervoort, J. D., Patchett, P. J., Blichert-Toft, J. & Albarede, F. Relationships between Lu-Hf and Sm-Nd isotopic systems in the global sedimentary system. *Earth Planet. Sci. Lett.* **168,** 79–99 (1999).
29. Scherer, E. E. *et al.* Lu-Hf geocheonology applied to dating Cenozoic events affecting lower crustal xenoliths from Kilbourne Hole, New Mexico. *Chem. Geol.* **142,** 63–78 (1997).
30. Gurnis, M., Mueller, R. D. & Moresi, L. Cretaceous vertical motion of Australia and the Australian-Antarctic discordance. *Science* **279,** 1499–1504 (1998).
31. Kamenetsky, V. S. *et al.* Remnants of Gondwanan continental lithosphere in oceanic upper mantle; evidence from the South Atlantic Ridge. *Geology* **29,** 243–246 (2001).
32. Soffer, G., Goldstein, S. L., Graham, D. W., Langmuir, C. H. & Michael, P. J. An arctic mantle domain boundary: Evidence from the Gakkel Ridge. *Geochem. Cosmochim. Acta* **68,** A692 (2004).

Supplementary Information accompanies the paper on **www.nature.com/nature**.

Acknowledgements We are grateful for comments from D. Graham. We thank P. Tělouk for help with the Plasma 54. This work was supported by the National Science Foundation and the Institut National des Sciences de l'Univers.

Competing interests statement The authors declare that they have no competing financial interests.

Correspondence and requests for materials should be addressed to B.B.H. (Barry.Hanan@sdsu.edu).

The origin of the internal nostril of tetrapods

Min Zhu[1] **& Per E. Ahlberg**[2]

[1]*Institute of Vertebrate Paleontology and Paleoanthropology, Chinese Academy of Sciences, P.O. Box 643, Beijing 100044, China*
[2]*Department of Evolutionary Organismal Biology, Evolutionary Biology Centre, Uppsala University, Norbyvägen 18A, SE-752 36 Uppsala, Sweden*

The choana, a unique 'internal nostril' opening from the nasal sac into the roof of the mouth, is a key part of the tetrapod (land vertebrate) respiratory system. It was the first component of the tetrapod body plan to evolve, well before the origin of limbs, and is therefore crucial to our understanding of the beginning of the fish–tetrapod transition. However, there is no consensus on the origin of the choana despite decades of heated debate[1–9]; some have claimed that it represents a palatally displaced external nostril[4,6], but others have argued that this is implausible because it implies breaking and rejoining the maxillary–premaxillary dental arcade and the maxillary branch of nerve V[2,6]. The fossil record has not resolved the dispute, because the choana is fully developed in known tetrapod stem-group members[8,10,11]. Here we present new material of *Kenichthys*, a 395-million-year-old fossil fish from China[12–14], that provides direct evidence for the origin of the choana and establishes its homology: it is indeed a displaced posterior external nostril that, during a brief transitional stage illustrated by *Kenichthys*, separated the maxilla from the premaxilla.

Most jawed fishes have anterior and posterior external nostrils but no connection between the nasal sac and mouth. The only living exception is the lungfishes, in which the posterior nostril is palatal, but this differs structurally from the tetrapod choana and is regarded as convergent[2,3,6]. Among those sarcopterygian fishes (lobe-fins) with a complete maxillary–premaxillary arcade, the nasal region comes in two patterns. In fishes belonging to the Tetrapodomorpha, the tetrapod total group[10–12], there is a single external nostril that lies between lateral rostral and tectal (Fig. 1f, g). On the palate, the anterior end of the maxilla splits into two diverging processes that surround a choana[3,15]. In non-tetrapodomorphs such as *Youngolepis*[16,17], which lack a choana (Fig. 1b, c), the anterior external nostril lies between the lateral rostral and tectal bones and the posterior nostril between the lateral rostral and lacrimal[3,9]. On the palate, the maxilla and premaxilla meet in a simple butt joint. *Kenichthys campbelli*, from the Emsian Chuandong Formation of Yunnan, China, presents the only known intermediate between these two patterns.

Kenichthys is the earliest known and most phylogenetically basal tetrapodomorph[11–14], a conclusion that we confirm here on the basis of a new expanded character suite (Supplementary Information). The snout and cheek bones of *Kenichthys*, including 19 ethmosphenoid and 10 maxilla specimens, are not preserved in articulation but are very well preserved and show little individual variation in morphology. This allows their positional relationships to be reconstructed with reasonable certainty, even though it is not possible to reassemble individual skulls (Figs 2 and 3). The anterior nostril occupies its usual position between lateral rostral and tectal (Fig. 1a, d). Unusually, however, the ventral margin of the lateral rostral extends some way beyond the posterior end of the premaxilla (Figs 1a, d, e and 2e). The end of the premaxilla is narrow and capped by cosmine (dentine with a thin enamel covering), without a sutural surface for the maxilla, and the free ventral edge of the lateral rostral is also cosmine-covered rather than sutural (Fig. 2a–h, j). It seems that these margins were free and wrapped in epithelium rather than sutured to the maxilla as in other lobe-fins. The small

14. Holstein, S. E., Ungewickell, H. & Ungewickell, E. Mechanism of clathrin basket dissociation: separate functions of protein domains of the DnaJ homologue auxilin. *J. Cell Biol.* **135,** 925–937 (1996).
15. Barouch, W., Prasad, K., Greene, L. & Eisenberg, E. Auxilin-induced interaction of the molecular chaperone Hsc70 with clathrin baskets. *Biochemistry* **36,** 4303–4308 (1997).
16. Takenaka, I. M., Leung, S. M., McAndrew, S. J., Brown, J. P. & Hightower, L. E. Hsc70-binding peptides selected from a phage display peptide library that resemble organellar targeting sequences. *J. Biol. Chem.* **270,** 19839–19844 (1995).
17. Schroder, S. *et al.* Primary structure of the neuronal clathrin-associated protein auxilin and its expression in bacteria. *Eur. J. Biochem.* **228,** 297–304 (1995).
18. Grigorieff, N. Three-dimensional structure of bovine NADH:ubiquinone oxidoreductase (complex I) at 22 Å in ice. *J. Mol. Biol.* **277,** 1033–1046 (1998).

Acknowledgements We are grateful to W. Boll and I. Rapoport for help in the purification of clathrin and adaptors, and to P. Sliz for advice on computational methods. This work was supported by grants from the NIH to T.K. and to D. De Rosier. N.G. and S.C.H. are investigators in the Howard Hughes Medical Institute.

Competing interests statement The authors declare that they have no competing financial interests.

Correspondence and requests for materials should be addressed to T.K. (Kirchhausen@crystal.harvard.edu). Coordinates have been deposited in the Protein Data Bank under accession number 1XI5.

corrigenda

The Ras–MAPK pathway is important for olfaction in *Caenorhabditis elegans*

Takaaki Hirotsu, Satoshi Saeki, Masayuki Yamamoto & Yuichi Iino

Nature **404,** 289–293 (2000).

In this Letter, we used strain MT2124, the standard *let-60(n1046gf)* strain maintained in the *Caenorhabditis* Genetics Center, for odour-chemotaxis assays. However, we have found that this strain carries a side mutation(s) that profoundly impairs chemotaxis to the odorant isoamyl alcohol, indicating that we need to re-evaluate our conclusion from the results shown in Fig. 1 that the *let-60(n1046gf)* mutant has a reduced efficiency of odorant chemotaxis. We outcrossed MT2124 to the wild-type N2 and obtained two *let-60(n1046gf)* strains, JN130 and JN131. We also outcrossed the MT4866 strain, the *let-60(n2021lf)* strain used in the study, and obtained the JN148 strain. All the outcrossed strains show reduced chemotaxis to the two odorants tested, isoamyl alcohol and diacetyl, at low odorant concentrations (T.H. and Y.I., unpublished results). The chemotaxis defects are comparable in extent to, or slightly weaker than, the original MT4866 *let-60(n2021lf)* strain. Our conclusion that both inactivation and hyperactivation of LET-60 Ras cause reduced chemotaxis therefore remains unchanged. However, the result shown in Fig. 1d, which suggested that *ksr-1(lf)*, *mek-2(lf)* and *mpk-1(lf)* suppress *let-60(n1046gf)*, is no longer valid because outcrossed *let-60(n1046gf)* strains do not show chemotaxis defects at the odorant concentration used in Fig. 1d (1×10^{-3} dilution of isoamyl alcohol). □

Contrasting origins of the upper mantle revealed by hafnium and lead isotopes from the Southeast Indian Ridge

Barry B. Hanan, Janne Blichert-Toft, Douglas G. Pyle & David M. Christie

Nature **432,** 91–94 (2004).

In this Letter, the quantity ε_{Hf} in Fig. 3 and its legend should read $\Delta\varepsilon_{Hf}$, which is the change in hafnium isotopic composition relative to the ε_{Nd}–ε_{Hf} mantle array. □